Structural Behavior of Reinforced Concrete Flat Plates Strengthened by Horizontal Reinforcement

Ali N. Ameen
Department of Civil Engineering, College of Engineering, University of Baghdad, Baghdad, Iraq
ali.nihad2101m@coeng.uobaghdad.edu.iq (corresponding author)

Mohannad H. Al-Sherrawi
Department of Civil Engineering, College of Engineering, University of Baghdad, Baghdad, Iraq
dr.mohannad.al-sherrawi@coeng.uobaghdad.edu.iq

Received: 14 March 2024 | Revised: 21 April 2024 and 19 May 2024 | Accepted: 20 May 2024

 DOI: https://doi.org/10.48084/etasr.7261

ABSTRACT

Flat plate structures consist of a slab supported directly by columns without beams or drop panels, resulting in a thinner slab with more efficient use of space. Despite these advantages, a flat plate slab is subjected to brittle punching shear. Sudden collapse may occur when a column pushes a piece of concrete from the slab above it. This paper displays Finite Element Analysis (FEA) using ABAQUS/ CAE 2019 to simulate the punching shear impact on a flat plate strengthened with horizontal steel bars of varying number and diameter, located at the compressive side of the slab. A numerical model was constructed with 8-noded hexahedral 3D brick elements for concrete and 2-noded linear 2D beam elements for steel reinforcement. The model was adapted based on experimental data. A parametric analysis was conducted to evaluate the impact of placing horizontal steel bars at the compression side of the flat plate and changing the quantity and size of these bars on the slab's performance. The results illustrate that the shear capacity increases from 17.07% to 28.13% as the bar diameter increases and from 19.17% to 54.82% as the number of bars increases.

Keywords-flat plates; punching shear; reinforced concrete; horizontal reinforcement; finite element analysis

I. INTRODUCTION

Punching shear results in unexpected failures of the flat plates, which can lead to catastrophic consequences [1, 2]. The punching shear of flat plates is influenced by several factors, for instance, shear and flexural reinforcement, boundary conditions, concrete strength, the ratio between the column and the slab, and the existence of openings [3-5]. Design codes address the problem of punching failure through various methods. The American standard ACI 318-19 [6] does not consider the impact of horizontal reinforcement, while the European standard Euro-Code2 [7] does. Depending on the design code, the critical area for punching can be half or twice the slab's effective depth calculated from the column's surface. Failures can be caused by the flexural punching mechanism resulting from local flexural yielding throughout the column [8]. Several studies have been conducted to enhance punching shear capacity through different techniques. Authors in [9] experimentally investigated 16 square specimens. Several materials and techniques, such as steel, GFRP, CFRP stirrups, and GFRP ropes, were used to enhance the punching capacity. Widths of 140 mm and 280 mm were utilized, along with different spacings between the stirrups (30, 50, and 70). The results demonstrated an enhancement in punching shear capacity, ranging from 3.13% to 74.67%. Authors in [10] assessed the precision of predicting the behavior of normal concrete in simulations of the punching shear strength of a flat slab. Finite element modeling in Abaqus was deployed, and the results were compared with those of other studies. Two concrete damage plasticity models were implemented, one with shear studs and one without. The finite element simulation provided very accurate findings. Broms [11], suggested installing stirrups and bent bars around the columns to prevent brittle punching failure. Authors in [12] conducted tests on seven flat slabs subjected to punching shear to study the influence of number, width, and spacing between stirrups and horizontal flexural reinforcement bars ratio. Authors in [13] utilized nonlinear finite element models to examine the punching shear behavior of flat slabs and analyze the influence of various factors. Authors in [14, 15] presented the experimental results on six square, reinforced concrete flat plates, strengthened by steel collars. In [16], a non-linear FEA study regarding strengthened flat plates using Z-shape shear reinforcement was conducted. Authors in [17] utilized the concrete damage plasticity model to examine five slab-column connections without shear reinforcement.

II. DESCRIPTION OF THE EXPERIMENTAL CONTROL SLAB

Authors in [18] tested an experimental sample that was employed to validate the presented model. The characteristics of concrete and steel rebars are summarized in Table I.

TABLE I. MATERIAL CHARACTERISTICS OF THE CONTROL SLAB.

Concrete's compressive strength [MPa]	Concrete's tensile strength [MPa]	Steel's yield strength [MPa]	Column's steel yield strength [MPa]	Yield strength of stirrups [MPa]
35	3.8	470	455	610

III. SIMULATION OF THE SLAB NUMERICAL MODEL

A Finite Element Analysis (FEA) numerical model was created to simulate the chosen slab sample using ABAQUS/ CAE 2019 [19]. The model retains spans from the actual test. A quarter of the flat plate slab was modeled in ABAQUS/CAE 2019, considering the geometry's symmetry, boundary conditions, and loading process [20]. Simple supports were placed 50 mm away from the edges. Symmetry criteria were implemented on internal surfaces, as indicated in Figure 1. The quasi-static dynamic/implicit test involves applying a controlled linear displacement to the upper surface of the column, with an ultimate limit of 20 mm. The ABAQUS/ CAE 2019 Concrete Damage Plasticity model was deployed. According to this model, concrete exhibits two distinct failure mechanisms: cracking and crushing [21, 22]. Table II displays the selected magnitude of variables for concrete plasticity damage properties. For the steel rebars, von Misses failure specification was applied. The assumption that the concrete and steel surfaces were perfectly bonded was made. Reduced-integration 8-noded hexahedral element (C3D8R) was adopted for concrete. A 2-noded linear beam in space (B31) was employed to model the steel element. Many mesh sizes were tested, and the 20 mm mesh size gave the most accurate results.

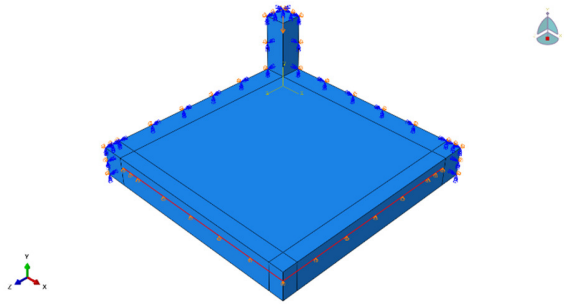

Fig. 1. Geometry and supports of the control slab.

TABLE II. CONCRETE PLASTICITY DAMAGE PROPERTIES

Dilation angle ψ	Eccentricity ε	Shape parameter Kc	Max. compression axial/biaxial	Viscosity μ
42	0.1	1.16	0.667	0.00002

IV. CALIBRATION VERIFICATION FOR THE SLAB MODEL

Load-deflection curves from the experimental test in [18] are compared to the slab model proposed in this research. The comparison is illustrated in Figure 2 and Table III, with S0 serving as the control sample.

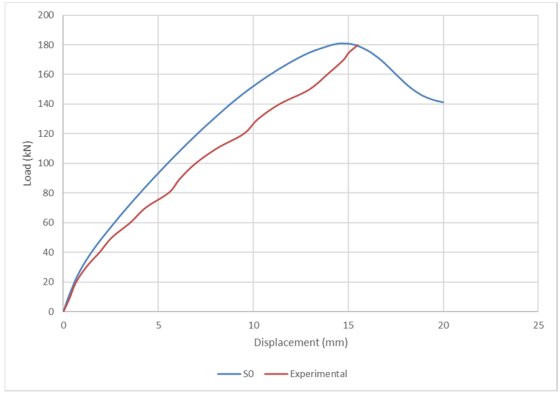

Fig. 2. Load-deflection relationship of the control slab.

This work precisely reflects the test outcomes of [18], as demonstrated in Table III. All the numerical curves were stiffer and more regular than the experimental curves due to the ideal and perfect conditions proposed by the finite element model, such as homogenous material, no shrinkage, and no slip between reinforcement bars and concrete. The relative inaccuracy for the ultimate load is 0.561%, and for the ultimate deflection is 6.129%. The contrast between the load-strain curves of concrete and steel of the experimental test derived by [18] and the slab model represented in this research can be observed in Figures 3 and 4.

TABLE III. DIFFERENCE BETWEEN THE EXPERIMENTAL AND THE FEA OUTCOMES OF THE CONTROL FLAT PLATE

Specimen ID	Ultimate Load (kN)		Ultimate Deflection (mm)		Discrepancy of P_u (%)
	Exp	FEA	Exp	FEA	
S0	180	181.01	15.5	14.55	0.561%

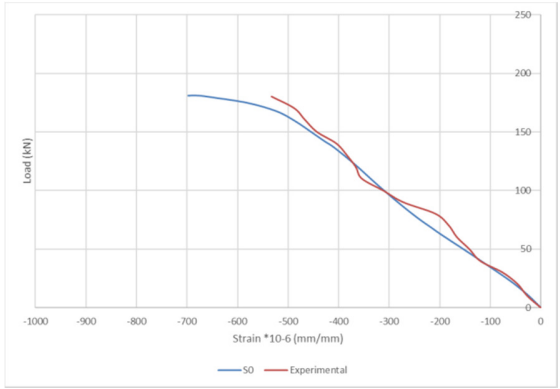

Fig. 3. Load-strain curves of the concrete of the control slab.

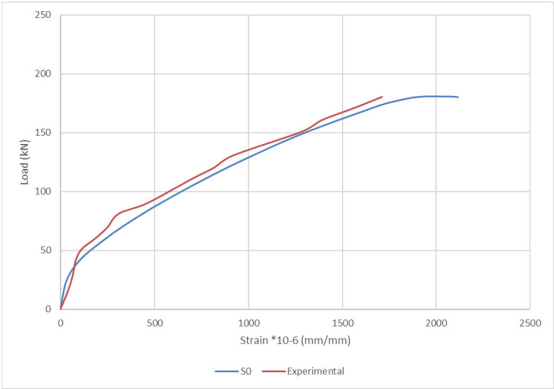

Fig. 4. Load-strain curves of the steel of the control slab.

The concrete's load-strain curve and the steel of the experimental test were measured at (d/2) from the surface of the column on the compression side for the concrete and the tension side for the steel. The comparison demonstrates an apparent convergence between FEA and experimental results. Both quantitative and qualitative calibrations were conducted. The cracking pattern in Figure 6 has been compared between numerical and experimental tests.

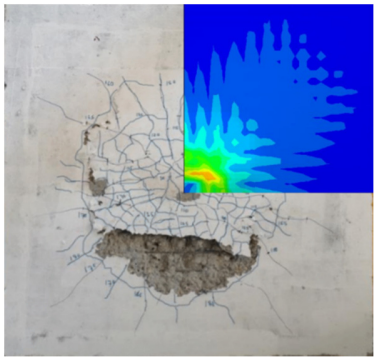

Fig. 5. Experimental and FEA crack pattern of the control slab.

V. PARAMETRIC STUDY AND RESULTS

Ten reinforced concrete slab specimens were divided into two groups (one for the study of the influence of the diameter of the horizontal steel bars and another for the study of the influence of the number of steel bars on the flat plate). Group one (S1, S2, S3, S4, and S5) specimens are reinforced with horizontal reinforcement with different diameters (12, 16, 20, 25, and 36 mm, respectively), with all specimens having 2 bars inserted in the slab. Group two (S6, S7, S8, S9, and S10) specimens are samples reinforced with horizontal reinforcement with different numbers of bars (1, 2, 3, 4, and 5 bars, respectively), with the bar diameter being 25 mm, and the development length of the additional bars being 750 (375 for the quarter model). Figure 6 shows the location of the additional bars.

Four categories were adopted in the result discussion to achieve a better understanding of the flat plate's structural behavior. These are:

1. Pattern of cracks and failure mode.
2. Load-deflection behavior with displacement stages, ultimate load, and displacement along the slab.
3. Load-strain behavior of concrete.
4. Load-strain behavior of steel with strain along the slab.

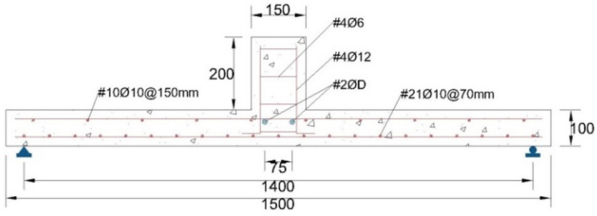

Fig. 6. Method of specimen strengthening.

A. *Pattern of Cracks and Failure Mode*

Every tested slab broke down brittlely. All specimens exhibited a typical punching shear angular cracking around the column. Group 1's crack patterns are portrayed in Figures 7-11. It can be noticed that the more the diameter increases, the more the cracks get distributed. The same thing goes for slabs S6 to S10. The cracks get distributed as the number of horizontal bars increases, which indicates that the slab's punching shear capacity is increasing. Figure 12 to Figure 16 depict the crack patterns of group 2.

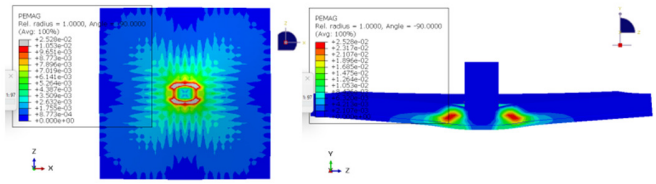

Fig. 7. Crack progression of S1.

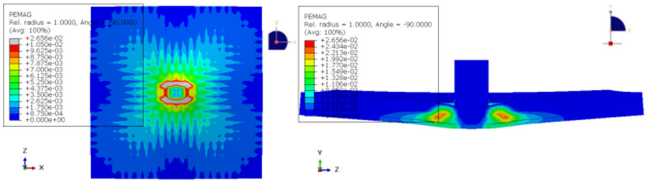

Fig. 8. Cracks progression of S2.

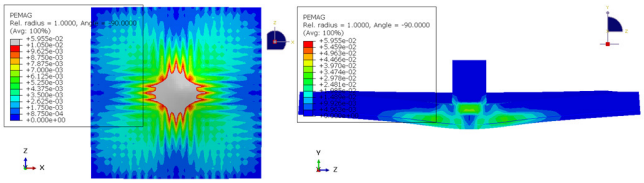

Fig. 9. Crack progression of S3.

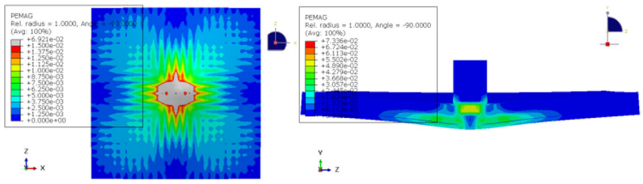

Fig. 10. Crack progression of S4.

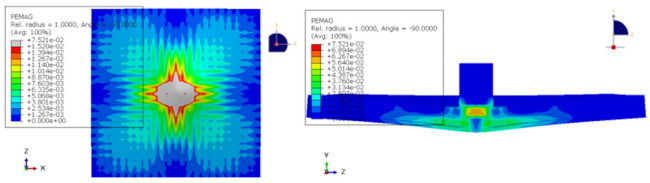

Fig. 11. Crack progression of S5.

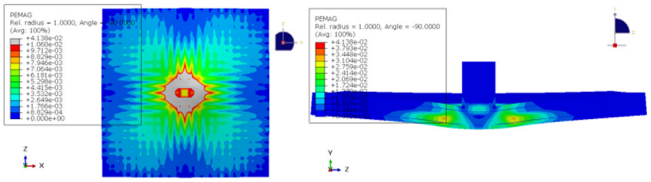

Fig. 12. Cracks progression of S6.

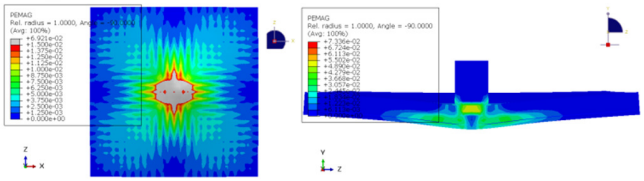

Fig. 13. Crack progression of S7.

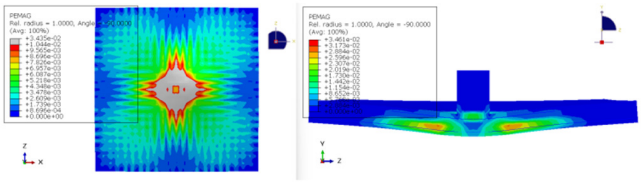

Fig. 14. Cracks progression of S8.

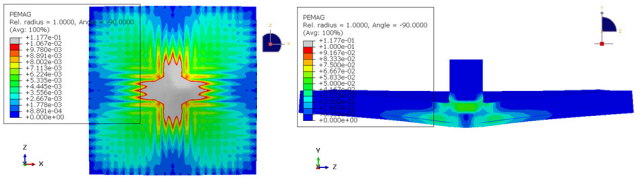

Fig. 15. Crack progression of S9.

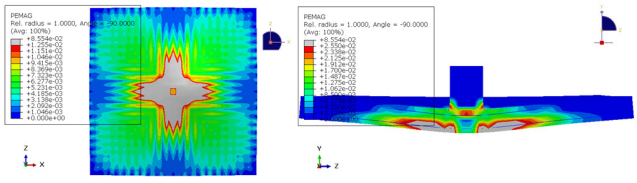

Fig. 16. Crack progression of S10.

B. Load-Deflection Bbehavior with Displacement Stages, Ultimate Load, and Displacement along the Slab

Vertical displacement was calculated at the middle span for each load increment of the test and every specimen. The control specimen has an initial cracking load P_{cr} of 41.44 kN, and the additional bars strengthen it by an amount of less than 0.01 kN; therefore, it was not taken into consideration, because the initial crack is formed at the tension side of the flat plate, whereas the additional bars are at the compressive side. Figure 17 illustrates the impact of the increasing diameter, while Figure 18 demonstrates the impact of the increasing number of bars on the load-deflection behavior at the center of the slab. All slabs are compared to the S0 specimen. Adding horizontal bars enhances the overall punching shear strength and the ductility of flat plates. The displacement of the first and second groups during all load stages is observed in Figures 19 and 20. Table IV exhibits each specimen's ultimate load and improvement percentage.

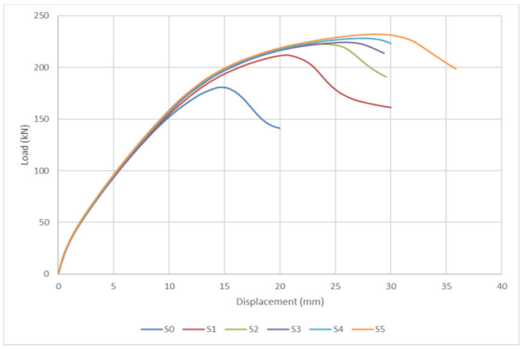

Fig. 17. Load-deflection curves of Group 1.

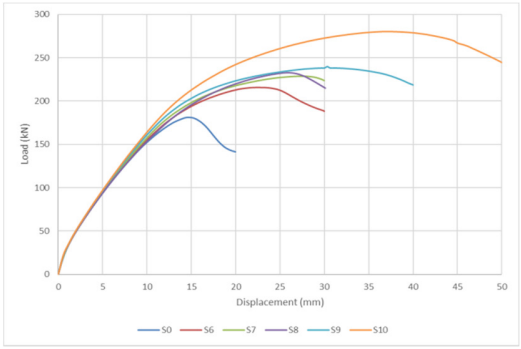

Fig. 18. Load-deflection curves of Group 2.

TABLE IV. ULTIMATE LOAD AND PERCENTAGE IMPROVEMENT OF GROUP 1 AND GROUP 2

Specimen ID	Ultimate Load (kN)	Improvement (%)
S1	211.91	17.07
S2	222.54	22.94
S3	224.29	23.91
S4	228.37	26.16
S5	231.93	28.13
S6	215.72	19.17
S7	228.37	26.16
S8	232.76	28.59
S9	239.79	32.47
S10	280.25	54.82

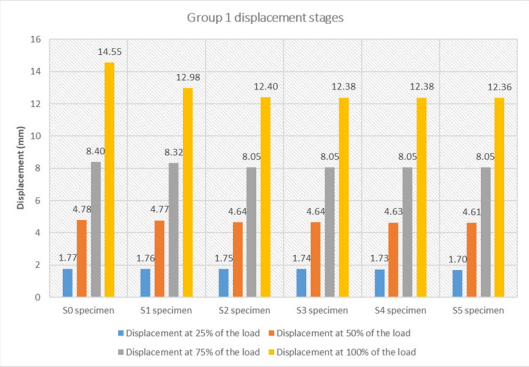

Fig. 19. Displacement stages of Group 1.

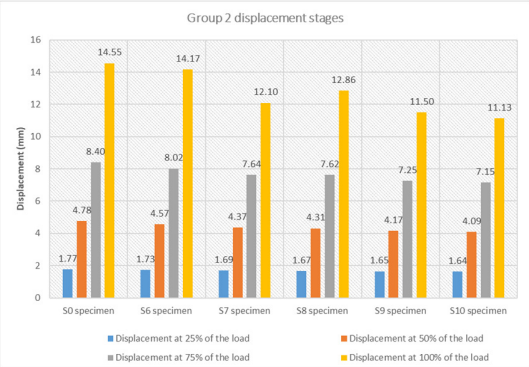

Fig. 20. Displacement stages of Group 2.

C. *Load-Strain Behavior of Concrete*

For both groups of specimens, the load-strain relationship was evaluated at d/2 from the column surface at the slab's concrete surface (compression side of the slab). Figure 21 shows how the diameter of bars impacts load-strain relations. In contrast, Figure 22 demonstrates the influence of increasing number of bars on the load-strain relations at the top surface of concrete, specifically at d/2 from the column's surface. Increasing the diameter and number of bars at the compression side of the slab exhibits a significant improvement in the load-strain behavior.

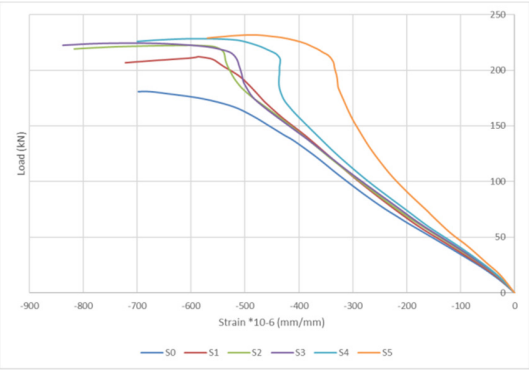

Fig. 21. Load-strain curves of concrete for Group 1.

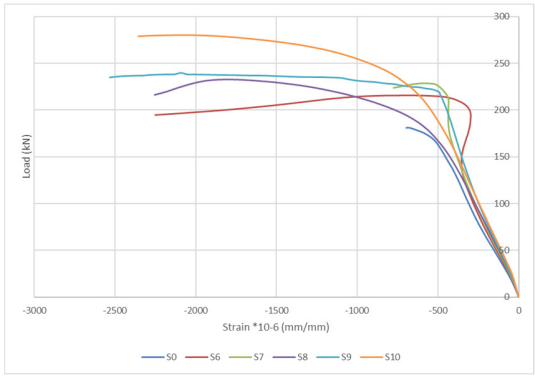

Fig. 22. Load-strain curves of concrete for Group 2.

D. *Load-Strain Behavior of Steel*

Figures 23 and 24 display the load-strain relationship of the flexural steel bar for groups one and two, respectively. The load-strain relationship was calculated at d/2 from the column's surface at one branch of the flexural tension bars.

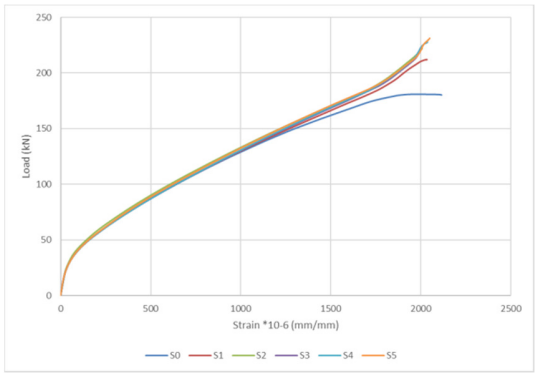

Fig. 23. Load-strain relationship of steel for Group 1.

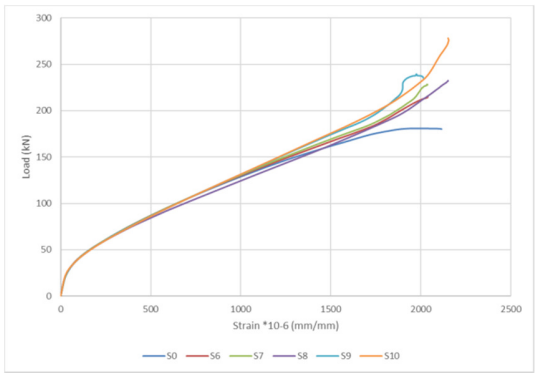

Fig. 24. Load-strain relationship of steel for Group 2.

It is evident that the strain, therefore the stress, decreases as the diameter and the number of bars increase. Figures 25-29 demonstrate the actual behavior of the steel strain along the slab as the applied load increases. The strain along the slab is investigated at 25%, 50%, 75%, and 100% of the ultimate load to fully reflect the behavior of the inserted steel along the slab during load application.

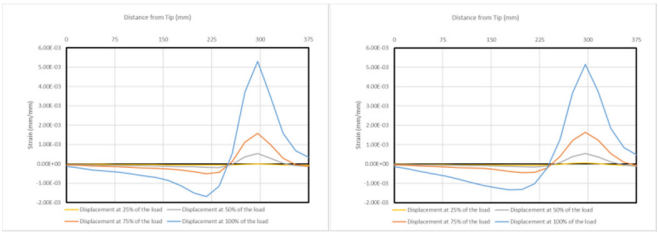

Fig. 25. Strain of steel along the slab of S1 and S2.

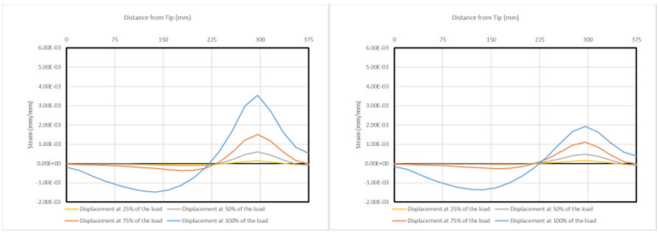

Fig. 26. Strain of steel along the slab of S3 and S4.

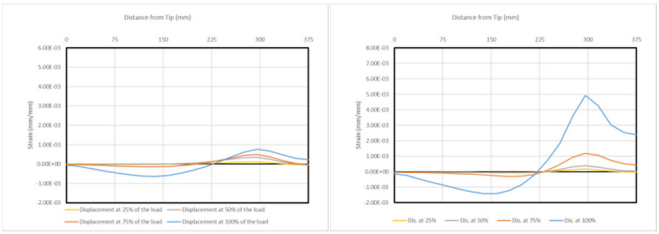

Fig. 27. Strain of steel along the slab of S5 and S6.

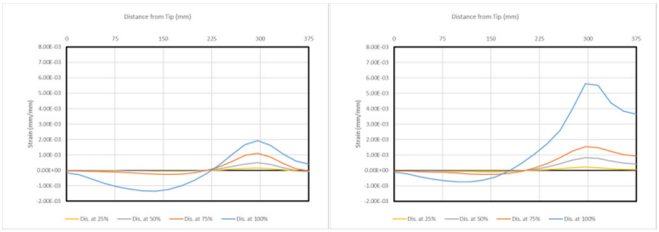

Fig. 28. Strain of steel along the slab of S7 and S8.

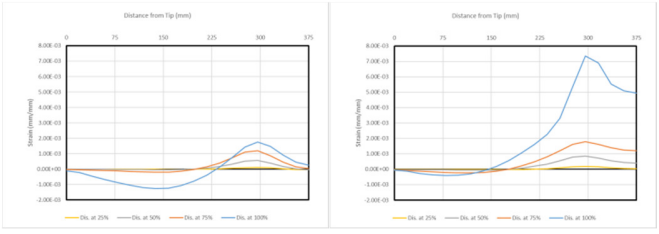

Fig. 29. Strain of steel along the slab of S9 and S10.

It can be noticed that the steel beneath the column is exposed to tension force because the column is penetrating the steel and the slab. From the face of the column onwards, it resists compression force because of its location for both groups. For the first group, the strain along the slab gets smaller as the diameter increases. For the second group, it can be noticed that the behavior varies because of the different distribution of even and odd numbers of bars.

VI. CONCLUSIONS

Finite element simulations were conducted in this paper using ABAQUS to analyze the punching shear in flat slab structures. The simulations were calibrated quantitatively and qualitatively based on experimental tests. Ten numerical models of flat plates made of reinforced concrete were tested under punching shear. The specimens are reinforced with horizontal bars at the flat plate's compression side with varying diameters and numbers. Based on the outcomes, several conclusions can be drawn:

1. Reinforcing the flat plates with horizontal bars at the compression side significantly increases the punching capacity of the flat plate slabs.
2. Increasing the diameter of bars enhances the punching shear capacity. Diameters of 12, 16, 20, 25, and 36 mm increased the bearing load by 17.07, 22.94, 23.91, 26.16, and 28.13%, respectively.
3. Increasing the number of bars enhances the punching shear capacity. Utilizing 1, 2, 3, 4, and 5 bars increased the bearing load by 19.17, 26.16, 28.59, 32.47, and 54.82%, respectively.

ACKNOWLEDGEMENT

The authors would like to gratefully present their acknowledgments to the Department of Civil Engineering at the University of Baghdad for the support received to achieve this work.

REFERENCES

[1] J. Moe, *Shearing strength of reinforced concrete slabs and footings under concentrated loads*. Skokie, Ill.: Portland Cement Association, Chicago, IL, USA:Research and Development Laboratories, 1961.

[2] S. King and N. J. Delatte, "Collapse of 2000 Commonwealth Avenue: Punching Shear Case Study," *Journal of Performance of Constructed Facilities*, vol. 18, no. 1, pp. 54–61, Feb. 2004, https://doi.org/10.1061/(ASCE)0887-3828(2004)18:1(54).

[3] A. H. H. Al-Shammari, "Effect of Openiings With or Without Strenghening on Punching Shear Strength for Reinforced Concrete Flat Plates," *Journal of Engineering*, vol. 17, no. 02, pp. 218–234, Apr. 2011, https://doi.org/10.31026/j.eng.2011.02.03.

[4] M. A. Golham and A. H. A. Al-Ahmed, "Strengthening of GFRP Reinforced Concrete Slabs with Openings," *Journal of Engineering*, vol. 30, no. 01, pp. 157–172, Jan. 2024, https://doi.org/10.31026/j.eng.2024.01.10.

[5] N. K. Oukaili and T. S. Salman, "Punching Shear Strength of Reinforced Concrete Flat Plates with Openings," *Journal of Engineering*, vol. 20, no. 01, pp. 1–20, Jan. 2014, https://doi.org/10.31026/j.eng.2014.01.01.

[6] ACI Committee 318, *318-19 Building Code Requirements for Structural Concrete and Commentary*. Farmington Hills, Michigan, USA: American Concrete Institute, 2019.

[7] *BS EN 1992-1-1:2023. Eurocode 2. Design of concrete structures - General rules and rules for buildings, bridges and civil engineering structures*. UK: BSI, 2023.

[8] S. K. Lakshmanaprabu, S. N. Mohanty, K. Shankar, N. Arunkumar, and G. Ramirez, "Optimal deep learning model for classification of lung cancer on CT images," *Future Generation Computer Systems*, vol. 92, pp. 374–382, Mar. 2019, https://doi.org/10.1016/j.future.2018.10.009.

[9] M. Makhlouf, G. Ismail, A. Kreem, and A. Marwa, "Investigation of transverse reinforcement for R.C flat slabs against punching shear and comparison with innovative strengthening technique using FRP ropes,"

Case Studies in Construction Materials, vol. 18, Feb. 2023, https://doi.org/10.1016/j.cscm.2023.e01935.

[10] Z. M. R. A. Rasoul and H. M. ali M.taher, "Accuracy of concrete strength prediction behavior in simulating punching shear behavior of flat slab using finite element approach in Abaqus," *Periodicals of Engineering and Natural Sciences*, vol. 7, no. 4, pp. 1933–1949, Dec. 2019, https://doi.org/10.21533/pen.v7i4.943.

[11] C. E. Broms, "Concrete Flat Slabs and Footings: Design Method for Punching and Detailing for Ductility," Ph.D. dissertation, KTH, Stockholm, Sweden, 2005.

[12] R. T. S. Mabrouk, A. Bakr, and H. Abdalla, "Effect of flexural and shear reinforcement on the punching behavior of reinforced concrete flat slabs," *Alexandria Engineering Journal*, vol. 56, no. 4, pp. 591–599, Dec. 2017, https://doi.org/10.1016/j.aej.2017.05.019.

[13] M. Navarro, S. Ivorra, and F. B. Varona, "Parametric computational analysis for punching shear in RC slabs," *Engineering Structures*, vol. 165, pp. 254–263, Jun. 2018, https://doi.org/10.1016/j.engstruct. 2018.03.035.

[14] A. A. Abdulhussein and M. H. Al-Sherrawi, "Experimental study on strengthening punching shear in concrete flat plates by steel collars," *AIP Conference Proceedings*, vol. 2651, no. 1, Mar. 2023, Art. no. 020026, https://doi.org/10.1063/5.0130802.

[15] A. A. Abdulhussein and M. H. Al-Sherrawi, "Experimental and Numerical Analysis of the Punching Shear Resistance Strengthening of Concrete Flat Plates by Steel Collars," *Engineering, Technology & Applied Science Research*, vol. 11, no. 6, pp. 7853–7860, Dec. 2021, https://doi.org/10.48084/etasr.4497.

[16] D.-A. Al-Jafar, H. Al Bremani, and A. Sagban, "Non-Linear Analysis to Improve Punching Shear Strength in Flat Slab Using Z-Shape Shear Reinforcement," vol. 7, pp. 65–70, Jan. 2019, https://doi.org/10.18081/ mjet/2019-7/65-70.

[17] A. S. Genikomsou and M. A. Polak, "Finite element analysis of punching shear of concrete slabs using damaged plasticity model in ABAQUS," *Engineering Structures*, vol. 98, pp. 38–48, Sep. 2015, https://doi.org/10.1016/j.engstruct.2015.04.016.

[18] A. N. Dalaf and S. D. Mohammed, "The Impact of Hybrid Fibers on Punching Shear Strength of Concrete Flat Plates Exposed to Fire," *Engineering, Technology & Applied Science Research*, vol. 11, no. 4, pp. 7452–7457, Aug. 2021, https://doi.org/10.48084/etasr.4314.

[19] *Abaqus/CAE User's Manual, version 6.8-1*. Hibbitt. Karlsson and Sorensen, Inc., 2015.

[20] G. A. Almashhadani and M. H. Al-Sherrawi, "Effect Change Concrete Slab Layer Thickness on Rigid Pavement," *Engineering, Technology & Applied Science Research*, vol. 12, no. 6, pp. 9661–9664, Dec. 2022, https://doi.org/10.48084/etasr.5283.

[21] D. C. Drucker and W. Prager, "Soil mechanics and plastic analysis or limit design," *Quarterly of Applied Mathematics*, vol. 10, no. 2, pp. 157–165, 1952, https://doi.org/10.1090/qam/48291.

[22] J. Lubliner, J. Oliver, S. Oller, and E. Oñate, "A plastic-damage model for concrete," *International Journal of Solids and Structures*, vol. 25, no. 3, pp. 299–326, Jan. 1989, https://doi.org/10.1016/0020-7683(89)90050-4.